3646–3653 *Nucleic Acids Research, 2007, Vol. 35, No. 11* *Published online 8 May 2007*
doi:10.1093/nar/gkm203

G-quadruplex formation in human telomeric $(TTAGGG)_4$ sequence with complementary strand in close vicinity under molecularly crowded condition

Zhong-yuan Kan[1], Yi Lin[2], Feng Wang[1], Xin-ying Zhuang[1], Yong Zhao[1], Dai-wen Pang[2], Yu-hua Hao[3] and Zheng Tan[1,3,*]

[1]Laboratory of Biochemistry and Biophysics, College of Life Sciences, [2]College of Chemistry and Molecular Sciences, Wuhan University, Wuhan 430072, P. R. China and [3]State Key Laboratory of Biomembrane and Membrane Biotechnology, Institute of Zoology, Chinese Academy of Sciences, Beijing 100080, P. R. China

Received November 4, 2006; Revised March 21, 2007; Accepted March 23, 2007

ABSTRACT

Chromosomes in vertebrates are protected at both ends by telomere DNA composed of tandem $(TTAGGG)_n$ repeats. DNA replication produces a blunt-ended leading strand telomere and a lagging strand telomere carrying a single-stranded G-rich overhang at its end. The G-rich strand can form G-quadruplex structure in the presence of K^+ or Na^+. At present, it is not clear whether quadruplex can form in the double-stranded telomere region where the two complementary strands are constrained in close vicinity and quadruplex formation, if possible, has to compete with the formation of the conventional Watson–Crick duplex. In this work, we studied quadruplex formation in oligonucleotides and double-stranded DNA containing both the G- and C-rich sequences to better mimic the *in vivo* situation. Under such competitive condition only duplex was observed in dilute solution containing physiological concentration of K^+. However, quadruplex could preferentially form and dominate over duplex structure under molecular crowding condition created by PEG as a result of significant quadruplex stabilization and duplex destabilization. This observation suggests quadruplex may potentially form or be induced at the blunt end of a telomere, which may present a possible alternative form of structures at telomere ends.

INTRODUCTION

Chromosomes in human cells are capped at both ends with non-coding tandem $(TTAGGG)_n$ DNA tracts called telomere. Telomere DNA plays important role in maintaining chromosome integrity and stability. They not only prevent the loss of coding information by buffering against the incomplete DNA replication, but also protect the natural chromosome ends from being recognized as double-stranded breaks (1). The DNA replication machinery produces two telomeres on each chromosome with different end structures, i.e. a blunt-ended leading strand telomere and a lagging strand telomere carrying a single-stranded 3′ G-rich overhang. The G-rich telomere overhang serves as substrate for telomerase that adds telomere repeats to telomere DNA and maintains telomere length homeostasis in germ lines and 85–90% of the tumor cells. The telomere overhang can also form distinct higher order structures (2). It can fold into a four-stranded structure called G-quadruplex (3) and inhibit telomerase activity (4). It can also swing back and invade the double-stranded telomere region to form circle-shaped t-loop structure (5).

Except the single-stranded overhang, the majority of the telomere DNA is double-stranded. It is not clear at present whether quadruplex can form in these regions. The formation of quadruplex in these regions would have to compete with the formation of the classical Watson–Crick duplex. Several *in vitro* studies have shown that the competition is affected by pH, temperature, cation species and strand concentration (6–10). All these studies were carried out using an inter-molecular system in which the G- and C-rich strands were free separate molecules and duplex was found to be the exclusive or dominant structure. As an inter-molecular reaction, the formation of duplex between two free complementary strands strongly depends on their concentration (10) and, as a result, quadruplex formed at very low strand concentration can be fully converted to duplex with increase in strand concentration (11). In cells, the two DNA strands in

*To whom correspondence should be addressed. Tel: +86 27 6875 4351; Fax: +86 27 6875 6661; Email: tanclswu@public.wh.hb.cn, z.tan@ioz.ac.cn

The authors wish it to be known that, in their opinion, the first three authors should be regarded as joint First Authors

chromosomes are well constrained in close vicinity. Therefore, the results obtained using separate G- and C-rich strands may not truly reflect the competition *in vivo*.

In this work, we studied quadruplex/duplex competition in an intra-molecular system in which the G-rich strand was linked via five thymines to the C-rich strand to better mimic the *in vivo* situation. Our data shows that the oligonucleotides only formed duplex in dilute solution containing physiological concentration of K^+ (150 mM). However, they preferentially formed quadruplex under molecular crowding condition, a reality of intracellular environment that has been shown recently to promote and stabilize quadruplex formation (9,12). The formation of quadruplex was confirmed by gel electrophoresis, fluorescent dye staining, circular dichroism (CD) spectroscopy and fluorescent polarization. To simulate the telomere end in chromosomes, we constructed double-stranded DNA (dsDNA) carrying four consecutive copies of TTAGGG/CCCTAA at one or both ends. Preferential quadruplex formation in the dsDNA was also observed under molecular crowding condition by atomic force microscopy (AFM) and gel electrophoresis. These results suggest that quadruplex might possibly form or be induced *in vivo* at the blunt-ended telomere termini as an alternative form of telomere end structures.

MATERIALS AND METHODS

Oligonucleotides

The 5′-$(CCCTAA)_nT_5(TTAGGG)_4$-3′ ($n = 4, 3, 2, 1, 0$) and relevant sequences (Table 1) were purchased from Sangon Biotech (Shanghai, China). Fluorescent 3′ FAM-labeled $(TTAGGG)_2TTA$ was purchased from TaKaRa Biotech (Dalian, China). In all experiments, oligonucleotides or DNAs were made in 10 mM Tris–HCl (pH 7.4) buffer containing 1 mM EDTA, 150 mM K^+ and 40% PEG 200 or no PEG, heated at 95°C for 5 min and cooled down to room temperature before use. In some experiments, oligonucleotides were labeled at the 5′ end with [γ-^{32}P]ATP using T4 polynucleotide kinase (Fermentas, Lithuania).

Double-stranded DNA

The dsDNAs (Ctrl-dsDNA and Telo-dsDNA) were obtained by polymerase chain reaction (PCR) from the pGEM plasmid. The telomere sequence (TTAGGG/CCCTAA)$_4$ at one or both end of the Telo-dsDNAs was introduced using $(CCCTAA)_4$-containing primers.

Gel electrophoresis

For the experiments in Figure 1, 5′-end-^{32}P-labeled oligonucleotides (~3 nM, 2000 c.p.m) were loaded onto 15% polyacrylamide gel containing 40% (w/v) PEG 200 or no PEG and electrophoresed at 4°C, 8 V/cm, in 1× TBE buffer containing 150 mM KCl. Gels were autoradiographed on a Typhoon phosphor imager (Amersham Biosciences, Sweden). For the experiments in Figure 2, electrophoresis were carried out as above and the oligonucleotides were visualized with ethidium bromide (EB) or 3,6-bis(1-methyl-4-vinylpyridinium)carbazole diiodide (BMVC). For the experiments in Figure 7, 100 ng (~1 pmol) dsDNA or 5′-^{32}P-labeled ssDNA was mixed with 100 pM mjaSSB, a 76 kDa single-stranded DNA-binding protein from archaeon *Methanococcus jannaschii* (13), loaded onto 8% polyacrylamide gel containing 40% (w/v) PEG 200, and electrophoresed at 4°C, 10 V/cm, in 1× TBE buffer containing 150 mM KCl. Gels for dsDNA were stained with EB. Samples prepared in PEG were run in PEG-containing gels. The DNAs were visualized by autoradiography or EB staining.

CD spectroscopy

The CD spectra of different oligonucleotides (5 μM) were collected from 320 to 220 nm on a CD6 spectropolarimeter (HORIBA Jobin Yvon, France) at 25°C with 1 mm pathlength cylinder quartz cuvette. CD-melting profiles

Table 1. Oligonucleotides used.

Oligonucleotide	Sequence
G4T4[a]	5′-$(T)_{24}$-$(T)_5$-$(TTAGGG)_4$-3′
G4C4R[b]	5′-AACCTCACACCTACCACTTCACAC-$(T)_5$-GTGTGAAGTGGTAGGTGTGAGGTT-3′
G4C4[c]	5′-$(CCCTAA)_4$-$(T)_5$-$(TTAGGG)_4$-3′
G4T3[a]	5′-$(T)_{18}$-$(T)_5$-$(TTAGGG)_4$-3′
G4C3R[b]	5′-ACACCTACCACTTCACAC-$(T)_5$-GTGTGAAGTGGTAGGTGTGAGGTT-3′
G4C3[c]	5′-$(CCCTAA)_3$-$(T)_5$-$(TTAGGG)_4$-3′
G4T2[a]	5′-$(T)_{12}$-$(T)_5$-$(TTAGGG)_4$-3′
G4C2R[b]	5′-ACCACTTCACAC-$(T)_5$-GTGTGAAGTGGTAGGTGTGAGGTT-3′
G4C2[c]	5′-$(CCCTAA)_2$-$(T)_5$-$(TTAGGG)_4$-3′
G4T1[a]	5′-$(T)_6$-$(T)_5$-$(TTAGGG)_4$-3′
G4T0[a]	5′-$(T)_5$-$(TTAGGG)_4$-3′
G4	5′-$(TTAGGG)_4$-3′
C4	5′-$(CCCTAA)_4$-3′
T_{29}	5′-$(T)_{29}$-3′
T_{24}	5′-$(T)_{24}$-3′

[a]They were designed to form G-quadruplex with a poly-T tail.
[b]They are designed to form hairpin duplex. The sequence at the right side of $(T)_5$ was randomized from $(TTAGGG)_4$ to abolish the ability of forming G-quadruplex. The underlined sequences at both side of $(T)_5$ are complementary to each other.
[c]The sequences can potentially form either G-quadruplex or hairpin duplex.

were recorded at 265 or 295 nm while temperature was increased at the rate of 1°C/min. Buffer blank correction was made for all measurements.

Fluorescence polarization

Fluorescence polarization measurements were carried out on a Spex Fluorolog-3 spectrofluorometer (HORIBA Jobin Yvon, France) at room temperature (20°C). $(TTAGGG)_2TTA$-FAM (50 nM) was incubated with each of the indicated oligonucleotide (100 nM) for 5 h at room temperature. Measurements were carried out using excitation and emission wavelength at 480 and 520 nm, respectively. For each sample, 10 parallel measurements with integration time of 2 s were averaged. Buffer blank was subtracted. Polarization values were calculated according to the equation $r = (I_{VV} - GI_{VH})/(I_{VV} + GI_{VH})$, where the first subscript indicates the orientation of the excitation polarization and the second of the emission polarization (V for vertical and H for horizontal). G is a calibrating factor related to the instrument settings calculated from $G = I_{HV}/I_{HH}$.

UV melting profile

The UV melting profiles were obtained on a DU-640 UV-VIS spectrophotometer (Beckman, Fullerton, CA, USA) equipped with a digital circulating water bath. The absorbance of oligonucleotides at 1 μM was monitored at 260 nm while temperature was simultaneously measured using a thermal probe immersed in the sample cell. The average heating rate was about 1°C/min.

Atomic force microscopy

Atomic force microscopy imaging was conducted with a Picoscan atomic force microscope (Molecular Imaging, Tempe, AZ, USA) (14). PCR product purified by gel electrophoresis was dissolved in 10 mM Tris (pH 7.4) containing 2 mM Mg^{2+} and 40% PEG 200 or no PEG. About 5 μl of DNA solution was dropped onto freshly cleaved ruby muscovite mica substrate (Digital Instruments, Santa Barbara, CA, USA). After 5 min, the mica surface was rinsed with ultrapure water and gently blew dry with nitrogen. Freshly prepared samples were mounted on AFM stage and imaged under MAC mode in air using Type II MAC Clever (spring constant = 0.95 N/m, Molecular Imaging, Tempe, AZ, USA). Typical scan rates were 1–3 Hz. The images were rastered at 512 × 512 pixels, unfiltered and flattened when needed.

RESULTS

Quadruplex formation in G-rich strand linked with C-rich strand

To better mimic the *in vivo* situation where the G- and C-rich strands of telomere DNA are constrained

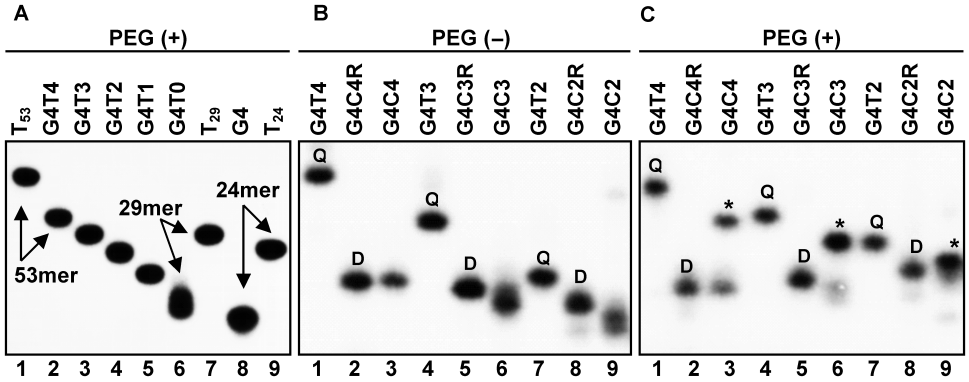

Figure 1. Autoradiograph of gels showing electrophoresis mobility of G4Cn and their reference oligonucleotides G4Tn and G4CnR ($n = 4, 3, 2, 1, 0$) prepared in 150 mM K^+ solution in the absence or presence of 40% (w/v) PEG 200. (**A**) The G4Tn formed quadruplex with a poly-T tail as indicated by their increased mobility relative to the size-matched references. (**B**) Structures formed in the absence of PEG. (**C**) New structural isoforms (asterisks) formed in G4Cn in the presence PEG, which are suggested to be quadruplex by their mobility relative to that of G4Tn and G4CnR. Q indicates the quadruplex formed by G4Tn and D the hairpin duplex by G4CnR, respectively. The calculated percentage of new species in G4C4 is 70%. Detailed sequence information is given in Table 1.

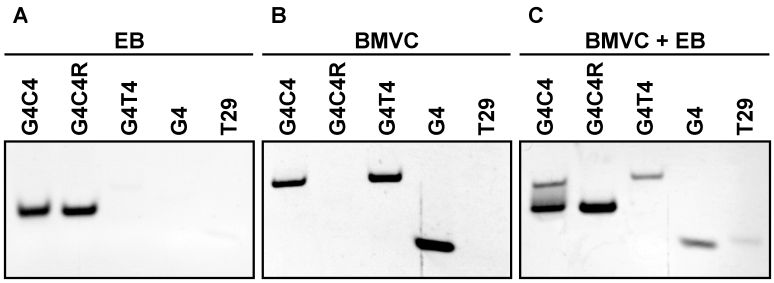

Figure 2. Oligonucleotides resolved by gel electrophoresis and visualized with fluorescent dye. Samples were prepared and electrophoresed in the presence of 40% (w/v) PEG 200 and 150 mM K^+. (**A**) Stained with ethidium bromide (EB), which is specific to duplex DNA. (**B**) Prestained with BMVC (1 μM), which is specific to human telomere quadruplex. (**C**) Same gel in (B), re-stained with EB.

in close proximity, we synthesized 5′-$(CCCTAA)_4$ $T_5(TTAGGG)_4$-3′ (named G4C4) and similar oligonucleotides. The structures of these oligonucleotides were studied in the absence and presence of 40% (w/v) PEG 200, an agent that has been used to mimic the molecularly crowded intracellular environment (15). In G4C4, the G-rich motif has the potential to either fold into G-quadruplex or form hairpin duplex with the C-rich motif. Two sequences, G4C4R and G4T4, designed to form duplex and G-quadruplex, respectively, were used as references (Table 1). The structures of these oligonucleotides were first examined by electrophoresis using ^{32}P-labeled oligonucleotides (Figure 1). Gel electrophoresis showed that $(TTAGGG)_4$ conjugated with non-complementary sequence of various length formed G-quadruplex in the presence of K^+ (Figure 1A). As judged from the mobility, the G4C4 formed duplex rather than G-quadruplex in the absence of PEG because it co-migrated with G4C4R that forms duplex, but migrated faster than the G4T4 that forms quadruplex (Figure 1B, lanes 1–3). In the presence of PEG, the G4C4 seems to have formed quadruplex as reflected by the appearance of a new band with mobility similar to that of the G4T4 (Figure 1C, lanes 1–3). From the intensity of the two bands, it is estimated that more than 70% of the G4C4 formed quadruplex. The formation of quadruplex became more dominant when the competition of duplex formation was reduced by decreasing the length of the complementary C-rich strand (Figure 1C, lanes 6, 9). In the absence of PEG, no quadruplex formation was observed in these oligonucleotides (Figure 1B), suggesting that quadruplex formation shown in Figure 1C was induced by PEG.

The structure of G4C4 in PEG solution was further verified by fluorescent dye staining with the reference oligonucleotides (Figure 2). EB, a dye for dsDNA, identified the duplex fraction in the G4C4, which had a same migration and staining efficiency as the duplex G4C4R (Figure 2A). BMVC is a carbazole derivative that preferentially stains the quadruplex formed by the human G-rich strand (16). When the samples were pre-stained with BMVC and resolved on gel, an alternative band was observed for the G4C4, which was as efficiently stained as the G4 and G4T4 that are known to form quadruplex. On the contrary, the duplex formed by G4C4R was not stained (Figure 2B). Post-staining of this gel with EB revealed the duplex bands of G4C4 and G4C4R below the quadruplex band of G4C4 (Figure 2C). This staining assay confirmed the observation in the gel electrophoresis that the G4C4 formed quadruplex in the presence of PEG.

The quadruplex formed by G4C4 in PEG solution was further analyzed by CD spectroscopy (Figure 3). In a separate work, we provided evidences by CD, gel electrophoresis, fluorescence spectroscopy of 2-aminopurine substituted oligonucleotides that the core sequence of the G-rich strand of human telomere DNA $(G_3T_2A)_3G_3$ adopts parallel-stranded conformation in 150 mM K^+ and 40% (w/v) PEG solution (manuscript submitted), which features a negative peak near 245 nm and a positive peak near 265 nm in CD spectrum as the many reported parallel-stranded quadruplexes (17–26). Here we decomposed G4C4 into three components, G4, C4 and T_5-linker, and recorded their CD spectrum separately. The G4 sequence alone produced a typical spectrum characteristic of parallel quadruplex with a negative peak near 245 and a positive peak near 265 nm. The G4C4 displayed a spectrum that is almost identical to the spectrum overlay of its composing components, G4, C4 and T5-linker (Figure 3A). Moreover, the spectrum of G4C4 resembled that of the G4T4 that forms quadruplex, but differed from that of the G4C4R that forms hairpin duplex (Figure 3B). In the majority of publications, it has been reported that anti-parallel quadruplex is characterized by a negative peak near 260 nm and a positive peak near 295 nm, while parallel quadruplex displays a negative peak near 240 nm followed by a positive peak near 265 nm (17,27,28). The CD analysis (Figure 3) suggests that the G4C4 adopted parallel quadruplex structure in the G-rich region as the G4. However, this conclusion regarding the folding topology may not be definitive because exceptions have been reported where anti-parallel quadruplex formed by some sequences also showed positive peak near 260 nm (29–31), typical of parallel quadruplex.

The PEG-induced formation of quadruplex in G4C4 should liberate the C-rich strand from base paring with the G-rich strand. This expected outcome was examined

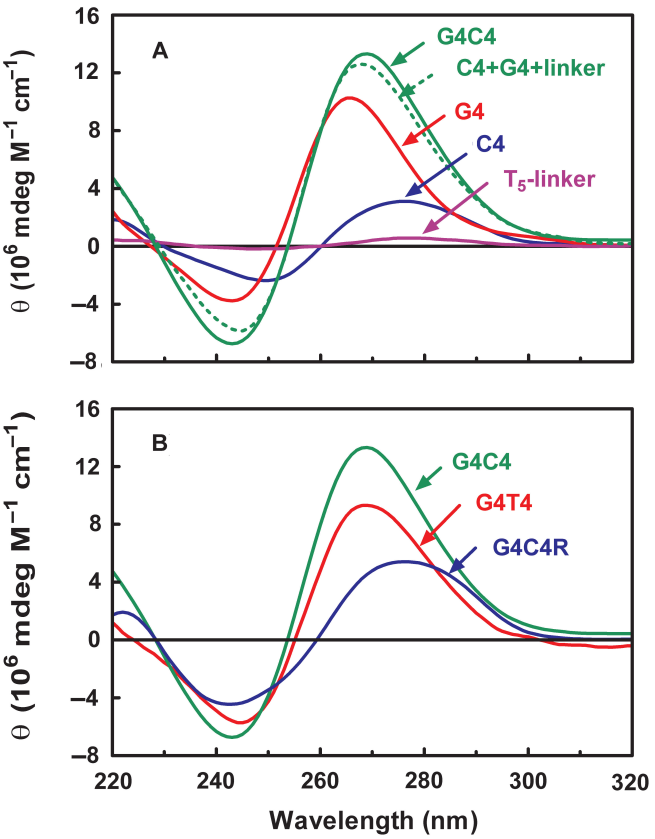

Figure 3. CD spectra of G4C4 and reference oligonucleotides in solution containing 150 mM K^+ and 40% (w/v) PEG 200. (**A**) CD spectra of G4C4 and its composing components. The spectrum of G4 + C4 + Linker gives the overlay of individual spectrum of G4, C4 and T_5-Linker. (**B**) CD spectra of G4C4, G4T4 and G4C4R. The later two oligonucleotides form quadruplex and hairpin duplex, respectively.

by a fluorescent probe $(TTAGGG)_2TTA$-FAM which is complementary to the C-rich strand (Figure 4). Upon binding to target strand, a probe is expected to show an increase in fluorescence polarization due to the decreased rotational freedom and this technique has been used in hybridization-based assays (32). In our work, the probe was added to solutions containing G4C4R, G4C4 and C4, respectively. In the absence of PEG, the probe only hybridized with the C4 as reflected by the increase in its fluorescence polarization but did not bind to the G4C4R and G4C4 since no change in its fluorescence polarization was detected. In the presence of PEG, the probe hybridized with both G4C4 and C4 resulting in an increase in polarization in both cases, indicating that the G4C4 formed quadruplex leaving the C-rich strand available to the probe.

Effect of molecular crowding on duplex and quadruplex formation

To examine how molecular crowding could affect the quadruplex and duplex formation separately, we studied the thermal stability of the two structures formed by G4T4 and G4C4R, respectively, in the absence and presence of PEG by thermal melting. Telomere quadruplex in K^+ solution without PEG is characterized by a positive peak at 295 nm in its CD spectrum (9), therefore the denaturation of quadruplex of G4T4 was monitored by CD at 295 and 265 nm, respectively, in the absence or presence of PEG. The denaturation of duplex is characterized by hyperchromicity at 260 nm (33) and was monitored by UV absorbance. The results in Figure 5A shows that the quadruplex formed by G4T4 was melted at 61.9°C in the absence of PEG, but was much more stable in the presence of PEG. On the other hand, PEG destabilized the duplex formed by G4C4R, resulting in a decrease of 14.5°C in melting temperature (Figure 5B). The effects of PEG on the stability of both structures is in agreement with the data reported in a recent work (12).

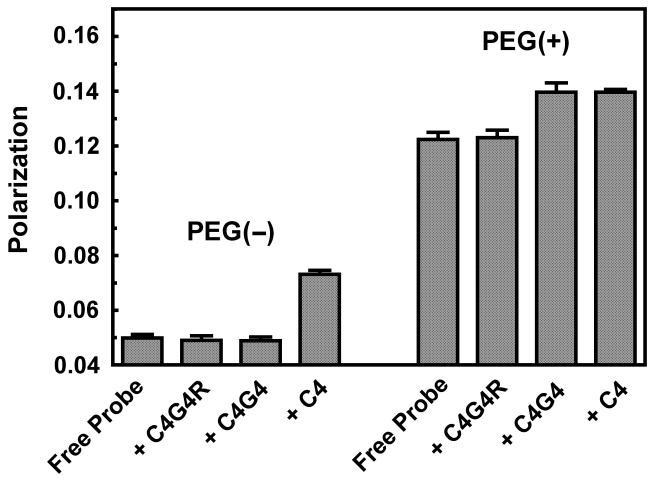

Figure 4. Fluorescence polarization of 3′ fluorescein-labeled $(TTAGGG)_2TTA$ probe incubated with different oligonucleotides in the absence or presence of 40% (w/v) PEG 200 in 150 mM K^+ solution.

Quadruplex formation in double-stranded DNA

To better simulate the telomere DNA in chromosomes, we constructed by PCR a 1.2 kb blunt-ended double-stranded DNA (Telo-dsDNA) carrying four consecutive copies of TTAGGG/CCCTAA at one end. Normal blunt-ended double-stranded DNA (Ctrl-dsDNA) containing no telomeric repeats was used as reference. The end structures of the dsDNAs were examined by AFM. Without PEG treatment, the two dsDNAs showed a typical shape of dsDNA edge at both ends (Figure 6A and B). In the presence of PEG, the formation of quadruplex could be recognized at one end of the Telo-dsDNAs as spherical dot (Figure 6C) with a height of 2.03 ± 0.48 nm which is similar to the reported values for quadruplex under AFM (34–36). The height of 0.65 ± 0.13 nm of the duplex region also matches those reported values for dsDNA (34,37).

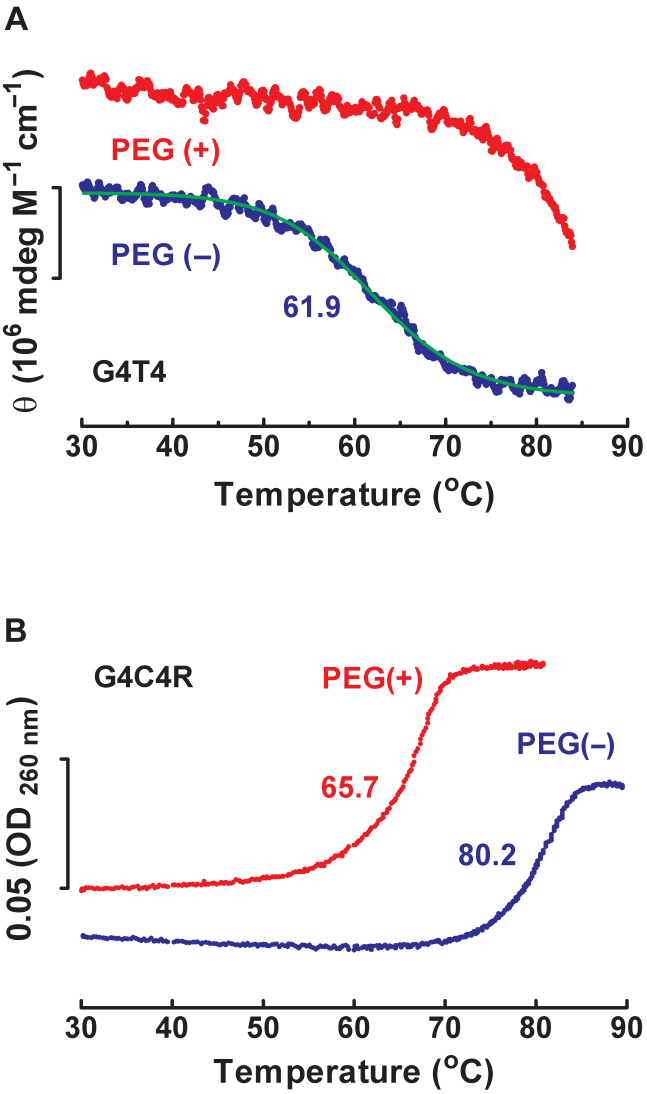

Figure 5. Thermal melting profiles of (**A**) G4T4 and (**B**) G4C4R in the absence and presence of 40% (w/v) PEG 200 in 150 mM K^+ solution. (**A**) CD-melting profile recorded at 265 nm in the presence or 295 nm in the absence of PEG. (**B**) UV melting recorded at 260 nm in the presence or absence of PEG. The numbers by the melting curves indicate the melting temperature T_m (°C) obtained in each measurement.

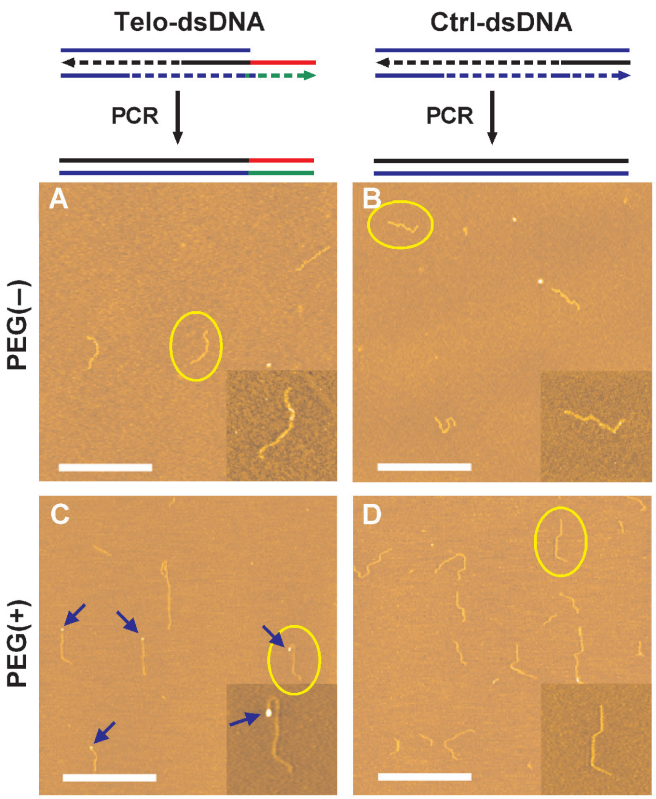

Figure 6. Atomic force microscopic images showing quadruplex formed in 1.2 kb double-stranded DNA in solution containing 150 mM K^+ and 40% (w/v) PEG 200. Arrowheads indicate quadruplexes. Insert at the right-bottom corner of each panel is the magnified rescan image of the DNA marked by oval. Bars = 1 μm. In (**C**) the average height of the quadruplexes is 2.03 ± 0.48 nm and that of duplex is 0.65 ± 0.13 nm.

Such structure was observed in the majority of the Telo-dsDNAs, but not seen in the PEG-treated Ctrl-dsDNA (Figure 6D).

The end structures of dsDNAs were also examined by gel electrophoresis. To increase sensitivity, a shorter dsDNA of 200 bp carrying four telomere repeats at both ends was constructed. The DNAs were incubated in PEG in the absence or presence of a 76 kDa single-stranded DNA-binding protein (SSB) before electrophoresis in PEG-containing gel. As judged from the mobilities, the SSB bound single-stranded DNA (ssDNA) (Figure 7A), but not the Ctrl-dsDNA (Figure 7B, lanes 3 and 4). In contrast, the Telo-dsDNA showed three distinct bands that can be explained by the formation of three different structures that had no quadruplex at both ends, had one quadruplex at one end or had quadruplex at both ends, respectively (Figures 7, lane 5). The two slower bands seemed to carry quadruplex. The formation of quadruplex at the end of the DNAs released the C-rich strand into single-stranded form, therefore SSB could bind to this strand and shifted the DNA to the much slower smears (Figure 7, lane 6).

DISCUSSION

The intracellular environment is crowded with high concentration of macromolecules whose total

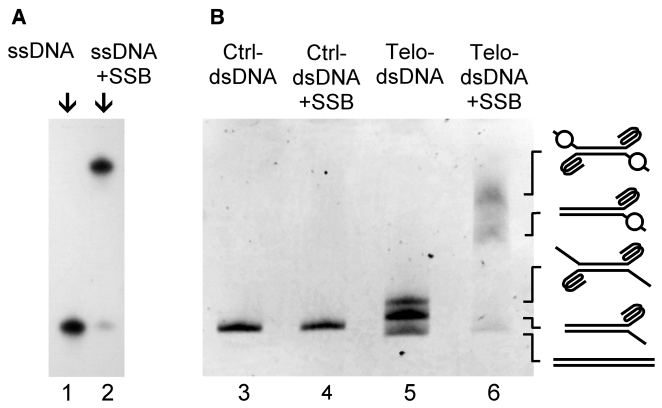

Figure 7. Gel electrophoresis showing quadruplex formation in double-stranded DNA in solution containing 150 mM K^+ and 40% (w/v) PEG 200 detected by a 76 kDa single-stranded DNA-binding protein (SSB). (**A**) The SSB shifted a 21 nt ssDNA. (**B**) The SSB did not shift the normal Ctrl-dsDNA but the Telo-dsDNA containing $(TTAGGG/CCCTAA)_4$ at both ends. The calculated intensity ratio of the three bands in lane 5 is 27.3/48.3/24.4 from which quadruplex was estimated to present at 51% of the ends. This should be an underestimated value since quadruplex and single-stranded DNA are not well stained by EB. Schematic drawings at the right represent the different structures. Circle indicates SSB.

concentration can reach 400 g/l (38). Studies have shown that molecular crowding induced transition from anti-parallel to parallel G-quadruplex (19), dissociation of duplex (23) in *Oxytricha nova* $G_4T_4G_4$ telomeric DNA, and transition from intra-molecular G-quadruplex to long multi-stranded G-wire in *Tetrahymena* $(T_2G_4)_3T_2G_2$ but not in human $G_3(T_2AG_3)_3$ telomeric DNA (24). Recently, we reported that molecular crowding can induce quadruplex formation under salt-deficient conditions and greatly enhance its competition with duplex formation in 150 mM K^+ solution using separate G- and C-rich strands (9). In this work, we extended the study using DNAs in which the C- and G-rich strands of human telomere DNA were kept in close proximity to better resemble the *in vivo* situation. In either the linked G- and C-rich strand or the dsDNAs, quadruplex was observed in the presence of PEG 200 (Figures 1–4, 6, 7). Moreover, the dominant quantity of quadruplex over that of duplex indicating that quadruplex was more competitive than duplex. Molecular crowding played a bifacial role in the competition by stabilizing quadruplex and, in the meantime, destabilizing duplex. While the hairpin duplex is more stable than quadruplex (T_m of 80.2 versus 61.9°C) in the absence of PEG, it became much less stable than the later (T_m of 65.7 versus ~>85°C) in the presence of PEG (Figure 5).

In our study, quadruplex was only observed when the DNAs were heat denatured to open the double stranded structure that was already present before the molecular crowding condition was applied. It is not clear whether such a structure can form *in vivo*. Quadruplex-forming sequences are present in many locations other than telomere in genomic DNA, for example, the promoter of BCL-2, retinoblastoma gene, hypoxia inducible factor 1α, *c-myc* oncogene [for review, see (39)]. So far, there are several evidences supporting the presence of telomere quadruplex in cells (40–45) which may occur at the single-stranded G-rich overhang. The question whether

quadruplex can form *in vivo* in the double-stranded region is not clear although the work on the promoter of the *c-myc* gene is consistent with quadruplex formation (46). The observed quadruplex formation in double-stranded telomere DNA in this work suggests it may potentially occur or be induced by exogenous molecules *in vivo* at least at telomere termini. In cells, the double-stranded telomere DNA is associated with several proteins such as TRF1 and TRF2 (47,48), which hold the DNA in place. However, the structure of dsDNA is dynamic. It has to be opened in many biological DNA-processing events, such as replication, transcription and promoter recognition. Spontaneous and transient openings of DNA duplex known as DNA breathing occur under physiological conditions which creates bubbles with size of up to few tens of base pairs (49). These events might provide opportunities for quadruplex to form at the blunt-ended telomere, which may present a possible alternative form of structures at telomere ends. Specific proteins may also participate to facilitate the opening of duplex or the formation of quadruplex. Small molecules that stabilize quadruplex or/and destabilize duplex may potentially induce such quadruplex formation, thus offer a possibility of manipulating the structure of double-stranded telomere DNA.

It is believed that the blunt-ended telomere produced by leading strand synthesis is processed afterwards to generate a single-stranded G-rich overhang (50), which is involved in the formation of t-loop that provides protection to the telomere end (51). Our observation of quadruplex formation at the blunt-ended telomere leaves several questions open that may deserve further exploration: whether the quadruplex could form under *in vivo* conditions; how would it affect the processing of the blunt telomere ends and what effect it would produce if the end-processing mechanism fails to produce single-stranded overhang under abnormal conditions.

ACKNOWLEDGEMENTS

This work was supported by grant Nos 2007CB507402 from MSTC, 20572082, 30670451 and the Science Fund for Creative Research Groups from NSFC. We thank Dr Ta-Chau Chang at the Institute of Atomic and Molecular Sciences, Academia Sinica, Taipei, Taiwan, ROC for providing the BMVC and Thomas J. Kelly at Johns Hopkins University School of Medicine, Baltimore, USA for providing the mjaSSB plasmid. Funding to pay the Open Access publication charges for this article was provided by the Science Fund for Creative Research Groups from NSFC.

Conflict of interest statement. None declared.

REFERENCES

1. Blackburn,E.H. (2001) Switching and signaling at the telomere. *Cell*, **106**, 661–673.
2. Neidle,S. and Parkinson,G.N. (2003) The structure of telomeric DNA. *Curr. Opin. Struct. Biol.*, **13**, 275–283.
3. Simonsson,T. (2001) G-quadruplex DNA structures – variations on a theme. *Biol. Chem.*, **382**, 621–628.
4. Zahler,A.M., Williamson,J.R., Cech,T.R. and Prescott,D.M. (1991) Inhibition of telomerase by G-quartet DNA structures. *Nature*, **350**, 718–720.
5. Griffith,J.D., Comeau,L., Rosenfield,S., Stansel,R.M., Bianchi,A., Moss,H. and de Lange,T. (1999) Mammalian telomeres end in a large duplex loop. *Cell*, **97**, 503–514.
6. Phan,A.T. and Mergny,J.L. (2002) Human telomeric DNA: G-quadruplex, i-motif and Watson-Crick double helix. *Nucleic Acids Res.*, **30**, 4618–4625.
7. Li,W., Wu,P., Ohmichi,T. and Sugimoto,N. (2002) Characterization and thermodynamic properties of quadruplex/duplex competition. *FEBS Lett.*, **526**, 77–81.
8. Li,W., Miyoshi,D., Nakano,S. and Sugimoto,N. (2003) Structural competition involving g-quadruplex DNA and its complement. *Biochemistry*, **42**, 11736–11744.
9. Kan,Z.Y., Yao,Y., Wang,P., Li,X.H., Hao,Y.H. and Tan,Z. (2006) Molecular crowding induces telomere G-quadruplex formation under salt-deficient conditions and enhances its competition with duplex formation. *Angew. Chem. Int. Ed. Engl.*, **45**, 1629–1632.
10. Kumar,N. and Maiti,S. (2005) The effect of osmolytes and small molecule on Quadruplex-WC duplex equilibrium: a fluorescence resonance energy transfer study. *Nucleic Acids Res.*, **33**, 6723–6732.
11. Zhao,Y., Kan,Z.Y., Zeng,Z.X., Hao,Y.H., Chen,H. and Tan,Z. (2004) Determining the folding and unfolding rate constants of nucleic acids by biosensor. Application to telomere G-quadruplex. *J. Am. Chem. Soc.*, **126**, 13255–13264.
12. Miyoshi,D., Karimata,H. and Sugimoto,N. (2006) Hydration regulates thermodynamics of G-Quadruplex formation under molecular crowding conditions. *J. Am. Chem. Soc.*, **128**, 7957–7963.
13. Kelly,T.J., Simancek,P. and Brush,G.S. (1998) Identification and characterization of a single-stranded DNA-binding protein from the archaeon Methanococcus jannaschii. *Proc. Natl Acad. Sci. USA*, **95**, 14634–14639.
14. Lu,Z.-X., Zhang,Z.-L., Zhang,M.-X., Xie,H.-Y., Tian,Z.-Q., Chen,P., Huang,H. and Pang,D.-W. (2005) Core/shell quantum-dot-photosensitized nano-TiO2 films: fabrication and application to the damage of cells and DNA. *J. Phys. Chem. B*, **109**, 22663–22666.
15. Chebotareva,N.A., Kurganov,B.I. and Livanova,N.B. (2004) Biochemical effects of molecular crowding. *Biochemistry (Mosc)*, **69**, 1239–1251.
16. Chang,C.C., Wu,J.Y., Chien,C.W., Wu,W.S., Liu,H., Kang,C.C., Yu,L.J. and Chang,T.C. (2003) A fluorescent carbazole derivative: high sensitivity for quadruplex DNA. *Anal. Chem.*, **75**, 6177–6183.
17. Balagurumoorthy,P., Brahmachari,S.K., Mohanty,D., Bansal,M. and Sasisekharan,V. (1992) Hairpin and parallel quartet structures for telomeric sequences. *Nucleic Acids Res.*, **20**, 4061–4067.
18. Chen,F.M. (1995) Acid-facilitated supramolecular assembly of G-quadruplexes in $d(CGG)_4$. *J. Biol. Chem.*, **270**, 23090–23096.
19. Miyoshi,D., Nakao,A. and Sugimoto,N. (2002) Molecular crowding regulates the structural switch of the DNA G-quadruplex. *Biochemistry*, **41**, 15017–15024.
20. Petraccone,L., Erra,E., Nasti,L., Galeone,A., Randazzo,A., Mayol,L., Barone,G. and Giancola,C. (2003) Effect of a modified thymine on the structure and stability of [d(TGGGT)](4) quadruplex. *Int. J. Biol. Macromol.*, **31**, 131–137.
21. Hardin,C.C., Henderson,E., Watson,T. and Prosser,J.K. (1991) Monovalent cation induced structural transitions in telomeric DNAs: G-DNA folding intermediates. *Biochemistry*, **30**, 4460–4472.
22. Jin,R., Gaffney,B.L., Wang,C., Jones,R.A. and Breslauer,K.J. (1992) Thermodynamics and structure of a DNA tetraplex: a spectroscopic and calorimetric study of the tetramolecular complexes of d(TG3T) and d(TG3T2G3T). *Proc. Natl Acad. Sci. USA*, **89**, 8832–8836.
23. Miyoshi,D., Matsumura,S., Nakano,S. and Sugimoto,N. (2004) Duplex dissociation of telomere DNAs induced by molecular crowding. *J. Am. Chem. Soc.*, **126**, 165–169.
24. Miyoshi,D., Karimata,H. and Sugimoto,N. (2005) Drastic effect of a single base difference between human and tetrahymena telomere sequences on their structures under molecular crowding conditions. *Angew. Chem. Int. Ed. Engl.*, **44**, 3740–3744.
25. Fernando,H., Reszka,A.P., Huppert,J., Ladame,S., Rankin,S., Venkitaraman,A.R., Neidle,S. and Balasubramanian,S. (2006)

A conserved quadruplex motif located in a transcription activation site of the human c-kit oncogene. *Biochemistry*, **45**, 7854–7860.
26. Cogoi,S. and Xodo,L.E. (2006) G-quadruplex formation within the promoter of the KRAS proto-oncogene and its effect on transcription. *Nucleic Acids Res.*, **34**, 2536–2549.
27. Giraldo,R., Suzuki,M., Chapman,L. and Rhodes,D. (1994) Promotion of parallel DNA quadruplexes by a yeast telomere binding protein: a circular dichroism study. *Proc. Natl Acad. Sci. USA*, **91**, 7658–7662.
28. Hazel,P., Huppert,J., Balasubramanian,S. and Neidle,S. (2004) Loop-length-dependent folding of G-quadruplexes. *J. Am. Chem. Soc.*, **126**, 16405–16415.
29. Dapic,V., Bates,P.J., Trent,J.O., Rodger,A., Thomas,S.D. and Miller,D.M. (2002) Antiproliferative activity of G-quartet-forming oligonucleotides with backbone and sugar modifications. *Biochemistry*, **41**, 3676–3685.
30. Dapic,V., Abdomerovic,V., Marrington,R., Peberdy,J., Rodger,A., Trent,J.O. and Bates,P.J. (2003) Biophysical and biological properties of quadruplex oligodeoxyribonucleotides. *Nucleic Acids Res.*, **31**, 2097–2107.
31. Jing,N., Rando,R.F., Pommier,Y. and Hogan,M.E. (1997) Ion selective folding of loop domains in a potent anti-HIV oligonucleotide. *Biochemistry*, **36**, 12498–12505.
32. Murakami,A., Nakaura,M., Nakatsuji,Y., Nagahara,S., Tran-Cong,Q. and Makino,K. (1991) Fluorescent-labeled oligonucleotide probes: detection of hybrid formation in solution by fluorescence polarization spectroscopy. *Nucleic Acids Res.*, **19**, 4097–4102.
33. Mergny,J.L., Phan,A.T. and Lacroix,L. (1998) Following G-quartet formation by UV-spectroscopy. *FEBS Lett.*, **435**, 74–78.
34. Marsh,T.C., Vesenka,J. and Henderson,E. (1995) A new DNA nanostructure, the G-wire, imaged by scanning probe microscopy. *Nucleic Acids Res.*, **23**, 696–700.
35. Miyoshi,D., Nakao,A. and Sugimoto,N. (2003) Structural transition from antiparallel to parallel G-quadruplex of d(G4T4G4) induced by Ca2+. *Nucleic Acids Res.*, **31**, 1156–1163.
36. Zhang,X.Y., Cao,E.H., Zhang,Y., Chou,C. and Bai,C. (2003) K(+) and Na(+)-induced self-assembly of telomeric oligonucleotide d(TTAGGG)(n). *J. Biomol. Struct. Dyn.*, **20**, 693–702.
37. Pietrasanta,L.I., Schaper,A. and Jovin,T.M. (1994) Probing specific molecular conformations with the scanning force microscope. Complexes of plasmid DNA and anti-Z-DNA antibodies. *Nucleic Acids Res.*, **22**, 3288–3292.
38. Zimmerman,S.B. and Trach,S.O. (1991) Estimation of macromolecule concentrations and excluded volume effects for the cytoplasm of Escherichia coli. *J. Mol. Biol.*, **222**, 599–620.
39. Kerwin,S.M. (2000) G-Quadruplex DNA as a target for drug design. *Curr. Pharm. Des.*, **6**, 441–478.
40. Schaffitzel,C., Berger,I., Postberg,J., Hanes,J., Lipps,H.J. and Pluckthun,A. (2001) In vitro generated antibodies specific for telomeric guanine-quadruplex DNA react with Stylonychia lemnae macronuclei. *Proc. Natl Acad. Sci. USA*, **98**, 8572–8577.
41. Chang,C.C., Kuo,I.C., Ling,I.F., Chen,C.T., Chen,H.C., Lou,P.J., Lin,J.J. and Chang,T.C. (2004) Detection of quadruplex DNA structures in human telomeres by a fluorescent carbazole derivative. *Anal. Chem.*, **76**, 4490–4494.
42. Duquette,M.L., Handa,P., Vincent,J.A., Taylor,A.F. and Maizels,N. (2004) Intracellular transcription of G-rich DNAs induces formation of G-loops, novel structures containing G4 DNA. *Genes. Dev.*, **18**, 1618–1629.
43. Granotier,C., Pennarun,G., Riou,L., Hoffschir,F., Gauthier,L.R., De Cian,A., Gomez,D., Mandine,E., Riou,J.F. *et al.* (2005) Preferential binding of a G-quadruplex ligand to human chromosome ends. *Nucleic Acids Res.*, **33**, 4182–4190.
44. Paeschke,K., Simonsson,T., Postberg,J., Rhodes,D. and Lipps,H.J. (2005) Telomere end-binding proteins control the formation of G-quadruplex DNA structures *in vivo*. *Nat. Struct. Mol. Biol.*, **12**, 847–854.
45. Chang,C.C., Chu,J.F., Kao,F.J., Chiu,Y.C., Lou,P.J., Chen,H.C. and Chang,T.C. (2006) Verification of antiparallel G-quadruplex structure in human telomeres by using two-photon excitation fluorescence lifetime imaging microscopy of the 3,6-bis(1-methyl-4-vinylpyridinium)carbazole diiodide molecule. *Anal. Chem.*, **78**, 2810–2815.
46. Siddiqui-Jain,A., Grand,C.L., Bearss,D.J. and Hurley,L.H. (2002) Direct evidence for a G-quadruplex in a promoter region and its targeting with a small molecule to repress c-MYC transcription. *Proc. Natl Acad. Sci. USA*, **99**, 11593–11598.
47. Yanez,G.H., Khan,S.J., Locovei,A.M., Pedroso,I.M. and Fletcher,T.M. (2005) DNA structure-dependent recruitment of telomeric proteins to single-stranded/double-stranded DNA junctions. *Biochem. Biophys. Res. Commun.*, **328**, 49–56.
48. de Lange,T. (2005) Shelterin: the protein complex that shapes and safeguards human telomeres. *Genes. Dev.*, **19**, 2100–2110.
49. Gueron,M., Kochoyan,M. and Leroy,J.L. (1987) A single mode of DNA base-pair opening drives imino proton exchange. *Nature*, **328**, 89–92.
50. Wei,C. and Price,M. (2003) Protecting the terminus: t-loops and telomere end-binding proteins. *Cell. Mol. Life Sci.*, **60**, 2283–2294.
51. de Lange,T. (2004) T-loops and the origin of telomeres. *Nat. Rev. Mol. Cell Biol.*, **5**, 323–329.